



**HAL**  
open science

## **Serum CD95L level correlates with tumor immune infiltration and is a positive prognostic marker for advanced high grade serous ovarian cancer**

Thibault de La Motte Rouge, Julien Corne, Aurelie Cauchois, Marie Le Boulch, Clotilde Poupon, Sebastien Henno, Nathalie Rioux-Leclercq, Estelle Le Pabic, Bruno Laviolle, Véronique Catros, et al.

### ► To cite this version:

Thibault de La Motte Rouge, Julien Corne, Aurelie Cauchois, Marie Le Boulch, Clotilde Poupon, et al.. Serum CD95L level correlates with tumor immune infiltration and is a positive prognostic marker for advanced high grade serous ovarian cancer. *Molecular Cancer Research*, 2019, 17 (12), pp.2537-2548. 10.1158/1541-7786.MCR-19-0449 . hal-02304765

**HAL Id: hal-02304765**

**<https://univ-rennes.hal.science/hal-02304765>**

Submitted on 4 Dec 2019

**HAL** is a multi-disciplinary open access archive for the deposit and dissemination of scientific research documents, whether they are published or not. The documents may come from teaching and research institutions in France or abroad, or from public or private research centers.

L'archive ouverte pluridisciplinaire **HAL**, est destinée au dépôt et à la diffusion de documents scientifiques de niveau recherche, publiés ou non, émanant des établissements d'enseignement et de recherche français ou étrangers, des laboratoires publics ou privés.

1  
2  
3  
4  
5  
6  
7  
8  
9  
10  
11  
12  
13  
14  
15  
16  
17  
18  
19  
20  
21  
22  
23  
24  
25

**Serum CD95L level correlates with tumor immune infiltration and is a positive prognostic marker for advanced high grade serous ovarian cancer**

Thibault De La Motte Rouge<sup>1, 2</sup>, Julien Corné<sup>1,2</sup>, Aurélie Cauchois<sup>3</sup>, Marie Le Boulch<sup>2</sup>, Clotilde Poupon<sup>2,4</sup>, Sébastien Henno<sup>2</sup>, Nathalie Rioux-Leclercq<sup>2</sup>, Estelle Le Pabic<sup>5</sup>, Bruno Laviolle<sup>5</sup>, Véronique Catros<sup>6</sup>, Jean Levêque<sup>2, 4</sup>, Alain Fautrel<sup>7</sup>, Matthieu Le Gallo<sup>1,2</sup>, Patrick Legembre<sup>1,2#</sup>, Vincent Lavoué<sup>2,4##\*</sup>

<sup>1</sup>Centre Eugène Marquis, Rennes, France.  
<sup>2</sup>INSERM, UMR 1242, COSS - Chemistry Oncogenesis Stress and Signaling, Rennes, France.  
<sup>3</sup>Department of Pathology, University Hospital of Rennes, Rennes, France.  
<sup>4</sup>Department of Gynecology, University Hospital of Rennes, Rennes, France.  
<sup>5</sup>Department of Biostatistics, University Hospital of Rennes, France.  
<sup>6</sup>Centre de Ressources Biologiques, CHU de Rennes.  
<sup>7</sup>Pathological Facility Platform, University of Rennes, France.

#Both of these authors made an equal contribution.

Authors have no potential conflicts of interest to disclose

**\*Corresponding author:** Prof. Vincent Lavoué, Vincent.lavoue@gmail.com, INSERM, UMR 1242, Chemistry Oncogenesis Stress and Signaling, Centre Eugène Marquis, Rue Bataille Flandres-Dunkerque, Rennes, France.

Running title: **Serum CD95L and tumor immune infiltration in ovarian cancer**



27  
28  
29

30 **Novelty & Impact Statements**

31 High levels of serum CD95L (s-CD95L) is correlated with the number of tumor-infiltrating  
32 immune cells in high grade serous ovarian cancer (HGSOC). These findings might therefore  
33 be used as a non-invasive marker of tumor immune infiltration. This would avoid tumor  
34 biopsy, which is difficult when a patient has relapsed. Immune checkpoint inhibitors such as  
35 PD-1/PD-L1 or CTLA4 antibodies are more effective in tumors with immune infiltration.  
36 Tomorrow, a personalized approach could be envisaged: after initial treatment, patients with  
37 HGSOC are tailored according to immune factors. Thus, s-CD95L as a surrogate of tumor  
38 immune infiltration could be used to select HGSOC patients referred for immunotherapy  
39 trials. Patients with low s-CD95L levels may be more appropriately directed to clinical trials  
40 using molecular therapies.

41  
42  
43

44 **Abstract**

45 Soluble CD95L (s-CD95L) is a chemoattractant for certain lymphocyte subpopulations. We  
46 examined whether this ligand is a prognostic marker for high grade serous ovarian cancer  
47 (HGSOC) and whether it is associated with accumulation of immune cells in the tumor.  
48 Serum s-CD95L levels in 51 patients with advanced ovarian cancer were tested by ELISA.  
49 Immunohistochemical staining of CD3, CD4, CD8, CD20, CD163, CD31, FoxP3, CCR6, IL-  
50 17, Granzyme B, PD-L1, and membrane CD95L was used to assess tumor-infiltrating  
51 immune cells. Although the intensity of CD3, CD8, CD4, CD20, and CD163 in tumor tissues  
52 remained constant regardless of membrane CD95L expression, tumors in HGSOC patients  
53 with s-CD95L levels  $\geq 516$  pg/ml showed increased infiltration by CD3+ T cells ( $p = 0.001$ ),  
54 comprising both cytotoxic CD8+ ( $p = 0.01$ ) and CD4+ ( $p = 0.0062$ ) cells including FoxP3+  
55 regulatory T cells ( $p = 0.0044$ ). Also, the number of tumor-infiltrating CD20+ B cells ( $p =$   
56  $0.0094$ ) increased in these patients. Multivariate analyses revealed that low s-CD95L  
57 concentrations ( $<516$  pg/mL, hazard ratio (HR), 3.54; 95% confidence interval (CI), 1.13–  
58 11.11), and  $< 1200$  activated CD8+ (Granzyme B+) cells (HR, 2.63; 95% CI, 1.16–5.95) were  
59 independent poor prognostic factors for recurrence, whereas  $>6000$  CD3+ cells (HR, 0.34;  
60 95% CI, 0.15–0.79) was a good prognostic factor. Thus, low levels of s-CD95L ( $<516$  pg/mL)  
61 are correlated with lower numbers of tumor-infiltrating lymphocytes (CD3+ and CD8+, but  
62 also CD4 and FoxP3 T cells) in advanced HGSOC and are a poor prognostic marker.

63 **Implications:** Serum s-CD95L is correlated with the number of tumor-infiltrating immune  
64 cells in HGSOC and could be used as a non-invasive marker of tumor immune infiltration to  
65 select patients referred for immunotherapy trials that evaluate checkpoint inhibitor treatment.

66

67

68

69

70 **Keywords:** High grade serous ovarian cancer; soluble CD95 ligand; tumor immune

71 infiltration

72

## 73 **Introduction**

74 Ovarian carcinoma is the seventh most common cancer in women and the eighth most common  
75 cause of cancer-related death worldwide <sup>1</sup>. At the time of diagnosis, the majority of patients  
76 with epithelial ovarian cancer (EOC) present with advanced disease, which is characterized by  
77 a high and widespread tumor load in the peritoneal cavity, often accompanied by malignant  
78 ascites. Thus, the prognosis of women with ovarian cancer remains poor, with a 5-year overall  
79 survival (OS) rate estimated at < 45% for all cancer stages, and only 20–30% for patients with  
80 Federation of Gynecologists and Obstetricians (FIGO) stage III or IV disease <sup>1,2</sup>.

81 Patients with EOC and other cancers who exhibit a robust immune response show increased  
82 survival rates <sup>3</sup>. Recent studies show that numbers of tumor-infiltrating lymphocytes (TILs),  
83 which are lymphocytes that extravasate from blood vessels to access the tumor, may be a  
84 positive predictive factor for melanoma <sup>4</sup>, colorectal cancer <sup>5</sup>, esophageal carcinomas <sup>6</sup>, breast  
85 cancer <sup>7,8</sup>, or endometrial cancer <sup>9</sup>. The presence of TILs affects the outcome of ovarian  
86 cancer; high numbers of CD8<sup>+</sup> T cells in the immune infiltrate are associated with improved  
87 overall survival (OS) <sup>10-15</sup>, particularly in patients with high grade serous ovarian carcinoma  
88 (HGSOC) <sup>16-18</sup>. By contrast, clinical outcome of ovarian cancers infiltrated by regulatory  
89 FoxP3<sup>+</sup> T cells (Tregs) remains unclear; studies suggest either decreased OS <sup>19-21</sup> or improved  
90 clinical outcomes <sup>22-24</sup>. Furthermore, some works establish that ovarian cancer is often  
91 accompanied by systemic immunosuppression <sup>25,26</sup>, which correlates with a poor prognosis  
92 <sup>27,28</sup>. New treatment strategies based on neutralizing antibodies that target checkpoint  
93 inhibitors represent a revolution in the fight against cancer; indeed, such treatments have  
94 shown survival benefits in patients with melanoma <sup>29</sup> or lung cancer <sup>30</sup>. Therapeutic antibodies  
95 that block the PD1/PD-L1 checkpoint (such as nivolumab or pembrolizumab) or the CTLA4  
96 checkpoint (such as ipilimumab) show therapeutic responses linked to tumor immune  
97 infiltration <sup>31,32</sup>. Phase II studies of anti-PD1/PD-L1 therapy in ovarian cancer suggest that it

98 triggers anti-tumor responses<sup>33-35</sup>; and, several phases III studies are underway. In such cases,  
99 a serum theranostic biomarker would be useful for selecting patients that are eligible for  
100 immunotherapy trials.

101 CD95L (also called FasL), which belongs to the tumor necrosis factor family, binds to the  
102 receptor CD95 (also known as Fas). Whereas CD95 is ubiquitously expressed, CD95L shows  
103 a more restricted expression pattern; it is expressed mainly on the membrane of lymphocytes,  
104 where it plays a pivotal role in eliminating infected and transformed cells<sup>36</sup>. Binding of  
105 membrane-bound CD95L to CD95 recruits the adaptor protein Fas Associated Death Domain  
106 (FADD)<sup>37</sup>, which in turn aggregates caspase-8 and caspase-10 to induce apoptosis<sup>38</sup>. CD95L  
107 is also expressed by endothelial cells lining the blood vessels of patients with tumors and  
108 chronic inflammatory disorders<sup>39-41</sup>. These CD95L-expressing endothelial cells seem to  
109 behave as a selective immune barrier, killing CD8 T cells while being permissive for Treg  
110 cells<sup>41</sup>. CD95L can be cleaved by metalloproteases, thereby releasing soluble CD95L (s-  
111 CD95L) into the bloodstream. Binding of s-CD95L to CD95 fails to trigger cell death but  
112 rather induces a non-apoptotic signaling pathway that promotes the migration of T cells<sup>42</sup>.  
113 Here, we wondered whether s-CD95L plays a role in ovarian cancer and examined its impact  
114 on the immune landscape in HGSOC patients.

115

116 **Material and methods**

117 *Cell lines and culture conditions*

118 IGROV-1, OVCAR-3, OVCAR-8, and SKOV-3 cell lines were obtained from American  
119 Type Culture Collection (LGC Standards, Molsheim, France) and were authenticated by Short  
120 Tandem Repeat. Each month, routine testing was conducted on all cultured cells using the  
121 sensor-cell approach Plasmotest™ - Mycoplasma Detection Kit (InvivoGen). O170, O370,  
122 O386, and O829 cell lines were established in-house from primary solid tumor or  
123 carcinomatosis samples cut into small pieces (<1 mm<sup>3</sup>) with a scalpel and then subjected to  
124 enzymatic digestion with collagenase (0.23 Wünsch units/ml; Liberase™ research grade;  
125 Roche, Indianapolis, IN). These in-house cell lines had more than 20 passages. All cell lines  
126 were cultured in DMEM complete medium supplemented with L-glutamine and 8% fetal  
127 bovine serum. Cells were used within 6 months after resuscitation of frozen aliquots.

128 *Spheroid formation assays*

129 Cells (1000/well) were seeded in 96-well ultra-low attachment plates (Corning) and cultured  
130 for 7 days in serum-free culture medium (MammoCult™ Human Medium Kit, STEMCELL)  
131 supplemented with heparin (STEMCELL) and hydrocortisone (STEMCELL). At Day 7, the  
132 number of spheres per well was counted manually by taking five large field pictures of each  
133 well using a ×4 objective lens.

134 *Generation of cleaved CD95L*

135 HEK/293T cells cultured in 1% FCS-containing medium were transfected with 3 µg of empty  
136 plasmid or a wild-type CD95L-containing vector using the calcium/phosphate precipitation  
137 method. Medium containing s-CD95L and exosome-bound full-length CD95L was harvested  
138 5 days after transfection. Dead cells and debris were removed by centrifugation (2 × 4,500

139 rpm/15 min). Exosomes were pelleted by ultracentrifugation at 100,000 g for 2 h. Finally,  
140 debris- and exosome-free supernatants were concentrated (Centricon; 10 kDa cut-off) and  
141 dialyzed against PBS.

#### 142 ***Western blot analysis***

143 Cells were lysed for 30 min at 4°C in lysis buffer (25 mM HEPES pH 7.4, 1% v/v Triton X-  
144 100, 150 mM NaCl, 2 mM EGTA supplemented with a mix of protease inhibitors; Sigma-  
145 Aldrich). Protein concentration was determined using the bicinchonic acid method (PIERCE,  
146 Rockford, IL, USA). Proteins were separated on an 8% SDS-PAGE gel and transferred to a  
147 nitrocellulose membrane (GE Healthcare, Buckinghamshire, UK). The membrane was  
148 blocked for 30 min with TBST (50 mM Tris, 160 mM NaCl, 0.05% v/v Tween 20, pH 7.8)  
149 containing 5% w/v dried skimmed milk or bovine serum albumin (BSA) and incubated  
150 overnight at 4°C with primary antibodies (mouse anti-E-Cadherin, clone 36, BD Pharmingen;  
151 mouse anti-Vimentin, clone V9, DAKO; and mouse anti- $\alpha$ -actin, clone AC-74, Sigma)  
152 diluted in the same buffer used for saturation (milk for anti-E-cadherin and anti- $\alpha$ -actin  
153 antibodies and BSA for anti-vimentin antibodies). The membrane was washed with TBST,  
154 followed by incubation for 1 h with a peroxidase-conjugated anti-mouse antibody  
155 (SouthernBiotech, Birmingham, Alabama, USA). Proteins were visualized using the enhanced  
156 chemiluminescence substrate kit (ECL, GE Healthcare).

#### 157 ***Flow cytometry analysis***

158 Cells were stained for 30 min at 4°C with anti-CD24 (clone ML5, BD Pharmingen), CD44  
159 (clone G44-26, BD Pharmingen), and anti-CD95 (clone DX2, BD Pharmingen) monoclonal  
160 antibodies (mAbs). Isotype-matched murine fluorochrome-conjugated immunoglobulins (PE

161 mouse IgG2a, APC mouse IgG2b, and PE mouse IgG1, respectively; BD Pharmingen) were  
162 used as negative controls.

### 163 ***Quantitative real-time polymerase chain reaction***

164 Total RNA was extracted from the cells using the NucleoSpin<sup>®</sup> RNA Isolation Kit  
165 (Macherey-Nagel) and cDNA was generated from 1 µg of total RNA using the High-Capacity  
166 cDNA Reverse Transcription Kit (Applied Biosystems). Quality and quantity of total RNA  
167 and cDNA was measured using a DS-11 Spectrophotometer (DeNovix). Expression of mRNA  
168 was measured using the TaqMan Gene Expression Assay Kit (Applied Biosystems), which  
169 contains primers and TaqMan MGB probes specific for the following genes: FAP1 (assay #:  
170 Hs00196632\_m1), ZEB1 (Hs00611018\_m1), ZEB2 (Hs00207691\_m1), CDH1  
171 (Hs00170423\_m1), SNAIL (Hs00195591\_m1), TWIST1 (Hs01675818\_s1), and human  
172 GAPDH (Hs99999905\_m1; endogenous control). The probes targeting SLUG  
173 (ENST00000020945.3|ENSG00000019549.9) were designed using the Universal Probe  
174 Library's Assay Design Center Tool (Roche), and the forward  
175 (TGGTTGCTTCAAGGACACAT) and reverse (GCAAATGCTCTGTTGCAGTG) primers  
176 were purchased from Eurogentec. Expression of SLUG mRNA was measured using  
177 PowerUp<sup>™</sup> SYBR<sup>™</sup> Green Master Mix (Applied Biosystems), with human GAPDH used as  
178 an endogenous control. Fifty nanograms of cDNA were used for each qPCR reaction. All  
179 qPCR experiments were performed in a QuantStudio5<sup>®</sup> machine (Applied Biosystems) and  
180 the data were analyzed using Thermo Fisher Connect<sup>™</sup> software (Thermo Fisher). Relative  
181 expression of each gene was calculated using the  $2^{-\Delta\Delta CT}$  method and expressed as a fold  
182 change.

### 183 ***Cell death assay***

184 Cell viability was measured in an MTT assay. Briefly,  $4 \times 10^4$  cells were cultured for 24 h in  
185 flat-bottom, 96-well plates along with the indicated concentrations of apoptosis inducer (final  
186 volume, 100  $\mu$ L). Next, 15  $\mu$ L MTT (5 mg/ml in PBS) solution was added and incubated at  
187 37°C for 4 h. Absorbance was measured using the Infinite F200 Pro (TECAN) at a  
188 wavelength of 570 nm.

### 189 ***Cell migration assay***

190 To determine whether s-CD95L contributed to T cell migration, T cells were exposed to s-  
191 CD95L or control medium in Boyden chambers. This migration assay was previously  
192 described<sup>43</sup>. Briefly, to measure trans-endothelial migration of activated T cells, use a 3  $\mu$ m-  
193 sized porous membrane of a Boyden chamber. HUVEC cells are plated to form a monolayer  
194 mimicking endothelial barrier. Membranes are first hydrated in sterile PBS, then, CD3/CD28-  
195 activated peripheral blood lymphocytes (PBLs) isolated from healthy donors ( $3 \times 10^5$   
196 cells/300  $\mu$ L) are added to the top chamber covered with a monolayer of HUVEC in a low  
197 serum (1%)-containing RPMI. Bottom chamber contains 500  $\mu$ L of RPMI 1% FBS in  
198 presence or absence of s-CD95L (100 ng/mL). Cells are cultured in a CO2 incubator at the  
199 same conditions as adherent cells for 24 h. Transmigrated cells are then counted in the lower  
200 reservoir.

### 201 ***Patients***

202 All clinical investigations were conducted in accordance with the principles outlined in the  
203 Declaration of Helsinki. Blood samples were collected from patients diagnosed with ovarian  
204 cancer after written informed consent was obtained. The study was approved by the local  
205 institutional review board (CEROG 2016-GYN-1003). Samples collected prospectively from  
206 patients diagnosed with ovarian cancer between January 2010 and December 2013 were

207 reviewed retrospectively. All samples were obtained at the time of diagnosis and before  
208 chemotherapy treatment. Fifty-one patients with advanced stage ovarian cancer were  
209 analyzed: 37 with HGSOC, six with endometrioid subtype, four with mucinous subtype, two  
210 with clear cell subtype, and two with low grade serous ovarian cancer. Thirty-six patients  
211 received neoadjuvant chemotherapy after tumor sample plus interval debulking surgery, and  
212 15 underwent primary debulking surgery followed by adjuvant chemotherapy. The surgical  
213 specimens were evaluated histologically at the Department of Pathology. All patients were  
214 staged according to the FIGO staging system<sup>44</sup>. After surgery, all patients received standard  
215 chemotherapy comprising carboplatin plus paclitaxel. For the current study, the main  
216 inclusion criterion was ovarian cancer with FIGO stage IIIC and IV (i.e., carcinomatosis stage  
217 or higher) and a serum sample in which the s-CD95L level before chemotherapy could be  
218 measured. Progression-free survival (PFS) was defined as the time from diagnosis of ovarian  
219 cancer to the time of recurrence or death. OS was defined as the time from diagnosis of  
220 ovarian cancer to the time of death. Observation time was defined as the interval between  
221 diagnosis and time of last contact (death or last follow-up). Data were censored at death or at  
222 the last follow-up for patients without recurrence.

### 223 ***Measurement of s-CD95L by ELISA***

224 S-CD95L concentrations in the serum of HGSOC patients and healthy donors were measured  
225 in an ELISA (Diaclone, Besançon, France). All blood samples were harvested at the time of  
226 diagnosis.

227

### 228 ***Tissue specimens and immunohistochemical staining***

229 Surgical specimens were fixed in 4% formalin, embedded in paraffin, and stained with  
230 hematoxylin-eosin-safran (HES). Sections from each histological specimen were reviewed by

231 two experienced pathologists (University Hospital, Rennes, France) to confirm the diagnosis  
232 and grade according to the method of Silverberg or Malpica (35). For each patient, a  
233 representative HES slide and the corresponding paraffin block were selected. The selected  
234 slide had to contain both tumor and adjacent stroma. The formalin-fixed paraffin-embedded  
235 blocks were cut into 5 µm slices and mounted on SuperFrost Plus microscope slides (Menzel  
236 Gläser, Braunschweig, Germany). Expression of CD3 (clone SP7; ThermoFisher, Brignais,  
237 France), CD4 (clone SP35; Cell Marque, Brignais, France), CD8 (clone C8/144B; DAKO,  
238 Les Ulis, France) CD20 (clone L26; DAKO), CD163 (clone 10D6; LEICA, Rungis, France),  
239 CD31 (clone JC70A; DAKO), Podoplanin (clone D2-40, INVITROGEN, Saint Aubin,  
240 France), FoxP3 (clone SP97; EUROBIO, Les Ulis, France), Granzyme B (clone GrB-7;  
241 Millipore), IL-17 (clone bs-2140R; BIOSS antibodies), and PD-L1 (clone E1L3N; Cell  
242 Signaling Technology) was assessed by immunohistochemistry (Ventana Discovery XT®  
243 automaton, Ventana Roche, Suisse). CD95L (clone G247-4, BD Pharmingen, France) was  
244 immunostained manually. After deparaffinization with toluene and rehydration with ethanol,  
245 sections were incubated at 95°C and bathed in Tris-EDTA at pH 8 prior to staining for CD4,  
246 CD8, FoxP3, CD20, CD3, CD31, CD163, CCR6, and Granzyme B. For CD95L, sections  
247 were deparaffinized and rehydrated, incubated at 95°C, and immersed in EDTA (pH 9). For  
248 all preparations, endogenous peroxidase activity was blocked by incubation in 0.3% hydrogen  
249 peroxide. The reactivity of all antibodies, except CD95L, was revealed with an HRP-labeled  
250 polymer-conjugated secondary antibody followed by diaminobenzidine (DAB; OmniMap  
251 DAB® Roche). CD95L was revealed with an anti-mouse HRP-labeled polymer-conjugated  
252 secondary antibody followed by DAB (DAB® Dako).

253

254 ***TIL count***

255 According breast cancer guidelines <sup>45</sup>, Tumour Infiltrating Lymphocytes can be subdivided  
256 according to their location within the tumor: 1) stromal TILs when located in the peritumoral  
257 space, and 2) intra-epithelial TILs, when they have penetrated the tumor islets. These  
258 recommendations are for breast cancer, and yet, there is no standardized approach to evaluate  
259 TILs in Epithelial Ovarian Cancer. Thus, in order to avoid a biased evaluation, we decided to  
260 perform a representative HES slide, which had to contain both tumor and adjacent stroma, in  
261 order to evaluate overall immune cells whatever their localization in tumor. Each  
262 immunostained slide was scanned with a NanoZoomer (HAMAMATSU). For each patient,  
263 five large field pictures were taken using a  $\times 5$  objective lens and HAMAMATSU's software  
264 (NDPview). All fields were analyzed using NIS-Elements software (Nikon) and positively  
265 stained cells were counted; for analysis, a specific threshold was applied for each antibody.

266

### 267 *Statistical analysis*

268 Statistical analysis was performed using SAS, v.9.4 (SAS Institute, Cary, NC, USA) and R  
269 logical Version 3.4.1 software programs. Quantitative results were expressed as the statistical  
270 mean  $\pm$  standard deviation and qualitative results as percentages (%). The Mann–Whitney–  
271 Wilcoxon test was used to compare the distribution of quantitative variables between two  
272 groups (abnormal statistical distributions). The Chi square or Fisher's exact test was used to  
273 compare the distribution of qualitative variables between two groups with theoretical  
274 headcounts  $< 5$ . The method of Contal and O'Quigley was used to determine cut-off values  
275 for the continuous variables used to examine prognosis <sup>46</sup>. The correlation between TILs and  
276 levels of cleaved CD95L was assessed using Spearman's correlation. The Kaplan–Meier  
277 method was used to compare survival curves between groups. All tests were two-sided and a  
278 p value  $< 0.05$  was deemed significant.

279

280 **Results**

281 **Serum CD95L is a prognostic marker for high grade serous ovarian cancer**

282 The clinical data and outcomes of our current HGSOC cohort match those of previously  
283 described cohorts,<sup>47,48</sup> indicating that, although the number of patients was relatively small,  
284 the cohort is likely to be representative of larger HGSOC cohorts (Table S1). In agreement  
285 with known clinical prognostic factors<sup>2,48,49</sup>, univariate analysis identified involved lymph  
286 nodes (HR, 4.87; 95% confidence interval (CI), 1.67–14.16) and residual disease after surgery  
287 (HR, 5.74; 95% CI, 2.40–13.74) as clinical parameters significantly associated with disease-  
288 free survival and OS (Table 3). Multivariate analysis revealed that residual disease after  
289 surgery (HR, 6.16; 95% CI, 2.27–16.67) correlated with recurrence rate (Table 4). Because  
290 we showed that serum CD95L is a poor prognosis marker in triple negative breast cancer  
291 women (26), we next investigated whether the concentration of serum CD95L in women with  
292 advanced ovarian cancer was associated with clinical outcome. Serum CD95L concentrations  
293 in ovarian cancer patients showed a more heterogeneous distribution than in healthy donors  
294 (Figure 1a), and there was no statistically significant difference between serum CD95L  
295 concentrations in ovarian cancer patients and healthy subjects (234,9.6 ±28.1 pg/mL vs. 359  
296 ±73.8 pg/mL, respectively).

297 The Contal and O’Quigley method<sup>46</sup> revealed that a serum CD95L concentration of 516  
298 pg/mL showed the strongest prognostic value for HGSOC patients (Figure 1c, e). We found  
299 that this cut-off failed to discriminate patients with long-term disease-free survival (DFS)  
300 from the whole population of ovarian cancer patients (Figure 1b). Nonetheless, for patients  
301 with HGSOC, this concentration discriminated poor-responders from long-term survival  
302 patients (Figure 1c). In agreement with this, the median concentration of s-CD95L in patients  
303 with DFS < 12 months was significantly lower than that in patients with a DFS >12 months  
304 (236 (0–480) vs. 317 (0–738), respectively; p=0.039); Figure 1d), and the OS of patients with

305 serum CD95L concentrations > 516 pg/ml was significantly longer than that of patients with a  
306 lower concentration (Figure 1e). Furthermore, univariate analysis pointed out that s-CD95L  
307 concentrations below 516 pg/mL were significantly correlated with node involvement (28%  
308 vs. 46%, respectively;  $p= 0.0409$ ) (Table 1) and node involvement is strongly associated with  
309 tumor relapse (Table 3).

310

### 311 **S-CD95L does not affect survival or proliferation of tumor cells or their sensitivity to** 312 **chemotherapy**

313 Because high concentrations of s-CD95L in HGSOE patients were associated with a better  
314 clinical outcome, we asked whether this ligand had a direct effect on death, proliferation,  
315 and/or differentiation of ovarian cancer cells. CD95 can induce cell death upon binding to  
316 membrane-bound CD95L (mCD95L)<sup>38</sup>. Therefore, we examined whether CD95L could kill  
317 ovarian cancer cells. All tested ovarian cancer cell lines (OVCAR-3, OVCAR-8, SKOV-3,  
318 and IGROV-1) and cells established from patients with HGSOE (O170, O370, O386, and  
319 O829) expressed CD95 (Supplementary data Figure 1a). These cells were classified as  
320 epithelial (OVCAR3, O370, O170, and 0386) or mesenchymal (O829, IGROV1, SKOV-3,  
321 and OVCAR-8) cells based on the vimentin/cadherin ratio (supplementary Figure 1b). Using a  
322 high s-CD95L concentration (*i.e.*, 100 ng/mL), we did not observe any cytotoxic effect of s-  
323 CD95L alone or in combination with doxorubicin and carboplatin chemotherapy drugs  
324 (Supplementary data Figure 2a and b).

325 Tumor heterogeneity is explained mainly by the hierarchical organization of tumor tissues, in  
326 which several subpopulations of self-renewing cancer stem cells (CSCs) sustain the long-term  
327 oligoclonality of the neoplasm<sup>50</sup>. Moreover, CSCs are thought to be the seeds required to  
328 establish distant metastasis, which is responsible for poor clinical outcome<sup>51</sup>. Addition of s-  
329 CD95L, with or without chemotherapy agents, did not affect the number of ovarian CSCs,

330 defined as CD24<sup>Low</sup>CD44<sup>High</sup>ALDH1<sup>+</sup> (Figure 2a, 2c and supplementary data Figure 2c).  
331 Moreover, neither the epithelial profile of OVCAR-3 nor the mesenchymal profile of  
332 OVCAR-8 varied in the presence of s-CD95L (Figure 2b). Finally, in all tested ovarian cancer  
333 cells, the rate of proliferation did not change in the presence of s-CD95L (Supplementary data  
334 Figure 1 d, e and f). Overall, these findings indicated that soluble CD95L has no effect on cell  
335 death, proliferation, or differentiation of ovarian cancer cells and does not enhance the anti-  
336 tumor effects of chemotherapeutic drugs. This leads to the hypothesis that s-CD95L may  
337 affect the tumor microenvironment, specifically the number/composition of immune tumor-  
338 infiltrating cells, in HGSOC patients.

339

#### 340 **Membrane CD95L is expressed on endothelial cells lining the blood vessels of HGSOC** 341 **tumors**

342 CD95L is expressed by endothelial cells lining the vessels of some ovarian cancers <sup>41</sup>.  
343 Therefore, we wondered whether this was also the case for HGSOCs. Immunohistochemical  
344 (IHC) analysis of tumor sections identified m-CD95L in 29 (79.2%) patients, but not in eight  
345 (20.8%). Using serial tumor slices, we validated that m-CD95L was expressed by CD31-  
346 expressing endothelial cells (Figure 3a), but not lymphatic endothelium (D2-40+).  
347 Interestingly, the intensity of m-CD95L expression in endothelial cells was correlated with the  
348 quantity of s-CD95L dosed in serum of these patients (supplementary Figure 3a, b). Of note  
349 (and unlike s-CD95L), we found no significant correlation between the intensity of staining  
350 for m-CD95L in tumor tissue and PFS or OS (table 3), suggesting that metalloprotease-  
351 mediated release of s-CD95L in ovarian cancers could exert an important biological function  
352 that impacts prognosis.

353

#### 354 **m-CD95L and the immune landscape in HGSOC**

355 Next, because tumor-infiltrating immune cells <sup>10,11,18</sup> are associated with a good clinical  
356 outcome in HGSOC, we examined tissues for the presence of tumor-infiltrating T cells  
357 (CD3/CD4/CD8/Th17), B cells (CD20), and macrophages (CD163). The cytolytic activity of  
358 CD8+ T cells was monitored by staining for Granzyme B. Checkpoint inhibitors are  
359 promising therapeutic regimens for HGSOC patients; therefore, we also stained tissues for  
360 PD-L1. Although the intensity of CD3, CD8, CD4, CD20, and CD163 markers did not change  
361 regarding the staining of membrane CD95L in tumor tissues, transmembrane CD95L  
362 expression was significantly associated with the number of tumor-infiltrating FoxP3 T cells  
363 (Table 2). This finding is in agreement with results published by Coukos et al <sup>41</sup>, who  
364 suggested that m-CD95L is a selective immune barrier; it killed CD8<sup>+</sup> cells but spared FoxP3-  
365 T cells. Nonetheless, we found no significant correlation between the intensity of m-CD95L  
366 staining and PFS or OS, indicating that unlike metalloprotease-cleaved s-CD95L, its  
367 membrane-bound counterpart is not a prognostic marker for HGSOC patients and that a yet  
368 unidentified metalloprotease plays a pivotal role in the disease progression. Because s-CD95L  
369 promotes T cell trafficking in lupus patients <sup>52</sup> (supplementary figure 4C) and expression of  
370 matrix-metalloproteinase-7 (MMP7) is higher in these patients <sup>53</sup>, MMP7 might be a good  
371 candidate for the metalloprotease involved in CD95L cleavage in HGSOC. Although the  
372 number of tumor-infiltrating CD8+ T cells did not correlate with the expression of m-CD95L,  
373 we found that the number of activated (GZB+) CD8+ T cells was higher in tumor tissues with  
374 greater expression of m-CD95L (Supplementary data Figure 3c). Because m-CD95L levels  
375 were not associated with a good prognosis, but activated (GZB+) CD8+ T cells were, this  
376 observation suggests immunosuppressive activity even in tumors showing high endothelial  
377 expression of m-CD95L.

378

379 **S-CD95L and the immune landscape in HGSOC**

380 Because high levels of serum s-CD95L are associated with a good prognosis in HGSOC  
381 patients, we next investigated whether the concentration of s-CD95L was associated with the  
382 number of TILs. We observed that the concentration of s-CD95L was correlated with the  
383 number of tumor-infiltrating CD3- and CD4-expressing T cells (Supplementary data Figure 4  
384 Panel A; CD3:  $r=0.4373$ ,  $p=0.0068$ ; CD4:  $r=0.3284$ ,  $p=0.0472$ ). Counterintuitively, the  
385 number of tumor-infiltrating Treg cells (FoxP3+) in HGSCO patients also correlated with s-  
386 CD95L expression ( $r=0.4584$ ,  $p=0.0043$ ); by contrast, the number of infiltrating IL17-  
387 producing Th17 cells did not (Figures 3b and supplementary data figure 4a). The number of B  
388 cells was associated significantly with the concentration of s-CD95L (Figure 3b and  
389 supplementary figure 4a). Finally, we found no correlation between s-CD95L levels and the  
390 number of tumor-infiltrating macrophages (CD163+ cells) (Figure 3b and supplementary  
391 figure 4a). Also, there was no correlation between s-CD95L and Granzyme B (a marker of  
392 CD8<sup>+</sup> T cell activation) or PD-L1 (Figure 3b and supplementary figure 4a), suggesting that s-  
393 CD95L is not involved in tumor recruitment/activation of cytolytic CD8<sup>+</sup> T cells (GZB) or  
394 expression of PD-L1, which contributes to exhaustion of CD3<sup>+</sup> T cells.

395 Overall, these findings suggested that the chemoattractant s-CD95L increases recruitment of  
396 CD8<sup>+</sup> T cells and Treg cells, among the CD4<sup>+</sup> T-cells, to HGSCO tumors, leading to an  
397 improved clinical outcome. Of note, we did not find any correlation between serum s-CD95L  
398 level and CD3<sup>+</sup> T-cell count in blood sample of HGSOC patients (supplementary data figure  
399 4, Panel b). To confirm that s-CD95L was able to promote cell motility of activated peripheral  
400 blood lymphocytes (PBLs), we incubated CD3/CD28-activated PBLs in the presence or  
401 absence of s-CD95L and evaluated cell migration using Boyden chambers. As shown in  
402 Figure 4, Panel c, s-CD95L enhanced the migration of activated T-cells.

403



405 **Discussion**

406 Here, we show that HGSOC patients with high levels of s-CD95L have a better prognosis  
407 than those with low levels. In addition, high s-CD95L levels correlate with increased numbers  
408 of tumor-infiltrating immune cells, including T-cells (CD8+ lymphocytes and Tregs), and B-  
409 lymphocytes. These findings suggest that s-CD95L plays a role in regulating tumor immune  
410 responses in women with HGSOC and could therefore be a non-invasive marker of tumor  
411 immune infiltration. Such a marker would avoid the need for tumor biopsy, which is difficult  
412 when a patient has relapsed. Immune checkpoint modulators such as PD-1/PD-L1 or CTLA4  
413 antibodies do not recruit lymphocytes, but break immunosuppression, which lead to restore  
414 cytotoxic T cell activity. Indeed, PD-1/PD-L1 blockade is more effective in tumors with  
415 immune infiltration. PD-1/PD-L1 antibodies trigger objective tumor responses in only 20–  
416 30% of patients with recurrent ovarian cancer <sup>34,35</sup>. So far, no biomarkers are associated  
417 strongly with high response rates, although PD-L1 expression on both tumor and immune  
418 cells can be used to select patients that are more likely to respond to PD1/PD-L1 treatment <sup>34</sup>.  
419 However, a pathology sample is needed to assess these biomarkers. Moreover, due to the  
420 heterogeneous nature of cancer, such a sample may not reflect the disease. Tomorrow, a  
421 personalized approach could be envisaged: after initial treatment, patients with HGSOC are  
422 tailored according to expression of immune factors. Thus, s-CD95L, as a surrogate marker of  
423 tumor immune infiltration, could be proposed to select HGSOC patients for immunotherapy  
424 trials: indeed, patients with high s-CD95L expression could be offered check point inhibitor  
425 treatment as a maintenance therapy, and patients with low s-CD95L expression may be more  
426 appropriately referred to clinical trials of chemotherapies. Nevertheless, a stronger efficiency  
427 of PD1/PD-L1 checkpoint inhibitor have still to be demonstrated for ovarian cancer patients  
428 with high infiltrate of immune cells as compared to women showing a low immune response.  
429 By now, the results of immunotherapy trials in ovarian cancer remain disappointing. Mesnage

430 et al. showed that neoadjuvant chemotherapy increases tumor immune infiltration in some  
431 HGSOC patients <sup>49</sup>; thus s-CD95L as a marker of tumor immune infiltration may allow us to  
432 monitor immune responses during neoadjuvant chemotherapy, and to select patients for  
433 immunotherapy when a strong tumor immune infiltrate is observed after neoadjuvant  
434 chemotherapy.

435 Although our data required an external validation with an independent cohort, one strength of  
436 the present study is that we selected only patients with HGSOC and FIGO III and IV stage  
437 (i.e., carcinomatosis stage or tumor peritoneal spread), which avoids confusion with other  
438 subtypes of ovarian cancer harboring different molecular mutations (e.g., mucinous,  
439 endometrioid, or clear cell ovarian cancer) and showing different immune responses <sup>54,55</sup>.  
440 Indeed, we observed no correlation between survival and s-CD95L levels in patients with  
441 HGSOC, mucinous, or endometrioid cancer. Furthermore, IHC experiments identified several  
442 types of immune cell in tumor tissue from these highly-selected patients: regulatory T cells  
443 (FoxP3 T cells), CD8 T cells, B cells (CD20 cells), and macrophages (CD163 cells). Zhang et  
444 al. showed a correlation between TIL numbers and OS and PFS<sup>11</sup>, as did Tomsova et al. <sup>13</sup>,  
445 Sato et al. <sup>10</sup>, and others <sup>56,57</sup>. Nevertheless, these studies suffer from lack of immune cell  
446 markers and heterogeneity. A counter-intuitive result is the better prognosis in patients with  
447 higher rate of tumor-infiltrating regulatory T cells (FoxP3 T cells). The magnitude of the  
448 immune reaction including tumor-infiltrating CD4+, CD8+ T cells and FosP3+ T-cells is  
449 associated with a better prognosis. Of note, in multivariate analysis, CD3+ and CD8+ T cells  
450 remain independent parameters associated with a better survival, while FoxP3 T cells is not  
451 (tables 4 and 5). It is also noteworthy that our IHC analysis fails to discriminate the different  
452 subsets of regulatory T cells. Indeed, recent data showed that regulatory T cells are  
453 heterogeneous, with five major structurally and genetically distinct cell subsets, each

454 representing a stage of maturation with distinct functional capacities, which could be pro-  
455 inflammation or tolerance<sup>58</sup>.

456 In other tumor models such as breast cancer, TILs can be subdivided according to their  
457 location within the tumor: stromal TILs when located in the peri-tumoral space, and intra-  
458 epithelial TILs, when they have penetrated the tumor islets. This classification was widely  
459 used in breast cancer and is now recommended in clinical routine<sup>45</sup>. Although these  
460 recommendations exist in breast cancer, there is no standardized approach to evaluate TILs in  
461 OC. In present study, we decided to perform a representative HES slide, which had to contain  
462 both tumor and adjacent stroma, in order to evaluate overall immune cells whatever their  
463 localization in tumor. Nonetheless, it would be interesting to perform in the future additional  
464 studies to address whether a correlation exists between TIL distribution and mCD95L  
465 expression or s-CD95L serum level. Because evaluation of tumor immune infiltration is  
466 difficult, the International Immuno-Oncology Biomarkers Working Group advocates  
467 evaluating intra-tumor lymphocytes in ovarian carcinoma using standard staining methods  
468 such as HES. They suggest a semi-quantitative evaluation of the area occupied by  
469 inflammatory mononuclear cells (lymphocytes and plasma cells, excluding  
470 polymorphonuclear cells)<sup>45</sup>. These recent recommendations suggest the need for a more  
471 reliable method of evaluating tumor immune infiltration and accordingly, we examined TILs  
472 in the recommended way using IHC. The serum concentration of s-CD95L may be a  
473 reproducible and simple tool for evaluating tumor immune responses in HGSOc patients.  
474 Furthermore, we found that s-CD95L is an independent prognostic factor of PFS in HGSOc  
475 ( $p = 0.0063$ ). HGSOc patients with high levels of s-CD95L show a good prognosis, which is  
476 opposite to that found for those with TNBC<sup>59</sup>. This discrepancy may be due to differences in  
477 tumor load, disease history (metastasis for TNBC and carcinomatosis for HGSOc), and  
478 different roles played by s-CD95L. In TNBC, s-CD95L triggers a pro-motile signal in tumor

479 cells, whereas in HGSOC it seems to contribute to the immune landscape through molecular  
480 mechanisms that remain to be elucidated.

481 Although we observed a correlation between expression of m-CD95L (assessed by IHC) in  
482 the tumor and serum s-CD95L levels in HGSOC patients, the eight patients lacking m-CD95L  
483 in the tumor still express s-CD95L in serum. This discrepancy could be due to intra-tumor  
484 heterogeneity; further studies are required to assess m-CD95L expression in a cohort from  
485 whom multiple biopsies are obtained from anatomically distinct sites. Another hypothesis  
486 could be that the membrane-bound ligand would already have been stripped from the  
487 endothelial cell surface.

488 Motz et al showed that m-CD95L on endothelial cells in ovarian cancer selectively killed  
489 cytotoxic CD8 T lymphocytes, without affecting FoxP3+ regulatory T lymphocytes; they  
490 postulated that CD95L expression on tumor endothelial cells is a poor prognostic factor due to  
491 this mechanism, which generates a tolerogenic microenvironment<sup>41</sup>. Our data suggest that the  
492 mechanism proposed by Motz et al. is not complete and that the CD95/CD95L system plays a  
493 more complex role in cancer. Indeed, we showed that s-CD95L is a good prognostic factor  
494 because it could contribute to drive anti-tumor immune responses; however, data obtained  
495 with m-CD95L confirm the results of Motz et al. in that a higher number of FoxP3 T cells are  
496 accumulated in tumors of patients with endothelial expression of m-CD95L as compared to  
497 those in which CD95L is not detected. The metalloprotease that cleaves m-CD95L to generate  
498 s-CD95L is the missing link that prevents us from presenting a more complete overview of  
499 HGSOC prognosis based on the CD95/C95L system. Nevertheless, our findings support the  
500 utility of s-CD95L as a biomarker for selecting HGSOC patients for checkpoint inhibitor  
501 treatment trial.

502

503 **Conclusion**

504 Serum concentration of s-CD95L is associated with an increased number of tumor-infiltrating  
505 FoxP3 T cells and a better prognostic in HGSOC women. S-CD95L levels correlate with  
506 prognosis. An s-CD95L level > 516 pg/mL is a cut-off value for assessing tumor immune  
507 infiltration in HGSOC patients and could be used to select patients for inclusion in clinical  
508 trials that evaluate checkpoint inhibitor treatment responses, such as inhibitors that block PD-  
509 1/PD-L1.

510

511 **List of abbreviations:**

512 HGSOC : high grade serous ovarian cancer

513 s-CD95L: serum CD95L

514 CD: cluster of differentiation

515 EOC: Epithelial ovarian cancer

516 OS: overall survival

517 PFS: Progression-free survival

518 FIGO: Federation of Gynecologists and Obstetricians

519 TIL: tumor-infiltrating lymphocytes

520 Tregs: regulatory FoxP3<sup>+</sup> T cells

521 FADD: Fas Associated Death Domain (FADD)

522 BSA: bovine serum albumin

523 HES: Hematoxylin-Eosin-Safran

524 DAB: Diaminodenzidine

525 CI: Confidence Interval

526 HR: Hazard Ratio

527 IHC: Immuno-Histo-Chemistry

528 MMP: metalloprotease

529 GZB: Granzyme B

530

531

532 **Declaration section:**

533

534 **Financial support:**

535 - The project was supported by La Vannetaise, Canceropole grand ouest (PLASTICO),

536 INCa PLBIO, Ligue Contre le Cancer, Fondation ARC and ANR PRCE.

537

538 **Conflict of interest statement:**

539

540 The authors declare no potential conflicts of interest.

541

542 **Data and material:**

543 All data and material are available.

544

545 **Agreement with publication and authors:**

546 All authors agree with this publication.

547

548 **Ethic statement**

549 This study was agreed by local institutional review board and French laws. All patients

550 consent to participate.

551

552 **Authors' contributions**

553 TDLMR, JC, AC, MLB, CP, PL and VL conceived and planned the experiments. TDLMR,

554 JC, AC, MLB, CP, and SH carried out the experiments. SH., NRL, ELP, BL, VC, JL, and

555 MLG contributed to sample preparation. TDLMR, SH, NRL, ELP, BL, PL and VL

556 contributed to the interpretation of the results. VL took the lead in writing the manuscript. All

557 authors provided critical feedback and helped shape the research, analysis and manuscript.

558

559 **Acknowledgements:**

560 Acknowledgements are due to "Centre de ressources biologiques du CHU de Rennes,

561 France".

562 Acknowledgements are due to "bioedits" for editing the draft.

## References

1. Webb PM, Jordan SJ. Epidemiology of epithelial ovarian cancer. *Best Pract Res Clin Obstet Gynaecol* 2017;41:3-14.
2. Vergote I, Trope CG, Amant F, et al. Neoadjuvant chemotherapy or primary surgery in stage IIIc or IV ovarian cancer. *N Engl J Med* 2010;363:943-53.
3. Chen DS, Mellman I. Oncology meets immunology: the cancer-immunity cycle. *Immunity* 2013;39:1-10.
4. Clemente CG, Mihm MC, Jr., Bufalino R, Zurrida S, Collini P, Cascinelli N. Prognostic value of tumor infiltrating lymphocytes in the vertical growth phase of primary cutaneous melanoma. *Cancer* 1996;77:1303-10.
5. Salama P, Phillips M, Grieu F, et al. Tumor-infiltrating FOXP3+ T regulatory cells show strong prognostic significance in colorectal cancer. *J Clin Oncol* 2009;27:186-92.
6. Schumacher K, Haensch W, Roefzaad C, Schlag PM. Prognostic significance of activated CD8(+) T cell infiltrations within esophageal carcinomas. *Cancer Res* 2001;61:3932-6.
7. Seo AN, Lee HJ, Kim EJ, et al. Tumour-infiltrating CD8+ lymphocytes as an independent predictive factor for pathological complete response to primary systemic therapy in breast cancer. *Br J Cancer* 2013;109:2705-13.
8. Yamaguchi R, Tanaka M, Yano A, et al. Tumor-infiltrating lymphocytes are important pathologic predictors for neoadjuvant chemotherapy in patients with breast cancer. *Hum Pathol* 2012;43:1688-94.
9. de Jong RA, Leffers N, Boezen HM, et al. Presence of tumor-infiltrating lymphocytes is an independent prognostic factor in type I and II endometrial cancer. *Gynecol Oncol* 2009;114:105-10.
10. Sato E, Olson SH, Ahn J, et al. Intraepithelial CD8+ tumor-infiltrating lymphocytes and a high CD8+/regulatory T cell ratio are associated with favorable prognosis in ovarian cancer. *Proc Natl Acad Sci U S A* 2005;102:18538-43.
11. Zhang L, Conejo-Garcia JR, Katsaros D, et al. Intratumoral T cells, recurrence, and survival in epithelial ovarian cancer. *N Engl J Med* 2003;348:203-13.
12. Zhang S, Ke X, Zeng S, et al. Analysis of CD8+ Treg cells in patients with ovarian cancer: a possible mechanism for immune impairment. *Cell Mol Immunol* 2015;12:580-91.
13. Tomsova M, Melichar B, Sedlakova I, Steiner I. Prognostic significance of CD3+ tumor-infiltrating lymphocytes in ovarian carcinoma. *Gynecol Oncol* 2008;108:415-20.
14. Stumpf M, Hasenburg A, Riener MO, et al. Intraepithelial CD8-positive T lymphocytes predict survival for patients with serous stage III ovarian carcinomas: relevance of clonal selection of T lymphocytes. *Br J Cancer* 2009;101:1513-21.
15. Lavoue V, Thedrez A, Leveque J, et al. Immunity of human epithelial ovarian carcinoma: the paradigm of immune suppression in cancer. *Journal of translational medicine* 2013;11:147.
16. Clarke B, Tinker AV, Lee CH, et al. Intraepithelial T cells and prognosis in ovarian carcinoma: novel associations with stage, tumor type, and BRCA1 loss. *Mod Pathol* 2009;22:393-402.
17. Townsend KN, Spowart JE, Huwait H, et al. Markers of T cell infiltration and function associate with favorable outcome in vascularized high-grade serous ovarian carcinoma. *PLoS One* 2013;8:e82406.

18. Pinto MP, Balmaceda C, Bravo ML, et al. Patient inflammatory status and CD4+/CD8+ intraepithelial tumor lymphocyte infiltration are predictors of outcomes in high-grade serous ovarian cancer. *Gynecologic oncology* 2018;151:10-7.
19. Curiel TJ, Coukos G, Zou L, et al. Specific recruitment of regulatory T cells in ovarian carcinoma fosters immune privilege and predicts reduced survival. *Nat Med* 2004;10:942-9.
20. Hermans C, Anz D, Engel J, Kirchner T, Endres S, Mayr D. Analysis of FoxP3+ T-regulatory cells and CD8+ T-cells in ovarian carcinoma: location and tumor infiltration patterns are key prognostic markers. *PLoS One* 2014;9:e111757.
21. Kryczek I, Wei S, Zhu G, et al. Relationship between B7-H4, regulatory T cells, and patient outcome in human ovarian carcinoma. *Cancer Res* 2007;67:8900-5.
22. Leffers N, Gooden MJ, de Jong RA, et al. Prognostic significance of tumor-infiltrating T-lymphocytes in primary and metastatic lesions of advanced stage ovarian cancer. *Cancer Immunol Immunother* 2009;58:449-59.
23. Milne K, Kobel M, Kalloger SE, et al. Systematic analysis of immune infiltrates in high-grade serous ovarian cancer reveals CD20, FoxP3 and TIA-1 as positive prognostic factors. *PLoS One* 2009;4:e6412.
24. Denkert C, von Minckwitz G, Darb-Esfahani S, et al. Tumour-infiltrating lymphocytes and prognosis in different subtypes of breast cancer: a pooled analysis of 3771 patients treated with neoadjuvant therapy. *Lancet Oncol* 2018;19:40-50.
25. Baert T, Vergote I, Coosemans A. Ovarian cancer and the immune system. *Gynecol Oncol Rep* 2017;19:57-8.
26. Turner TB, Buchsbaum DJ, Straughn JM, Jr., Randall TD, Arend RC. Ovarian cancer and the immune system - The role of targeted therapies. *Gynecologic oncology* 2016;142:349-56.
27. Huang QT, Zhou L, Zeng WJ, et al. Prognostic Significance of Neutrophil-to-Lymphocyte Ratio in Ovarian Cancer: A Systematic Review and Meta-Analysis of Observational Studies. *Cell Physiol Biochem* 2017;41:2411-8.
28. Wang Y, Liu P, Xu Y, et al. Preoperative neutrophil-to-lymphocyte ratio predicts response to first-line platinum-based chemotherapy and prognosis in serous ovarian cancer. *Cancer Chemother Pharmacol* 2015;75:255-62.
29. Wolchok JD, Chiarion-Sileni V, Gonzalez R, et al. Overall Survival with Combined Nivolumab and Ipilimumab in Advanced Melanoma. *The New England journal of medicine* 2017;377:1345-56.
30. Basak EA, Koolen SLW, Hurkmans DP, et al. Correlation between nivolumab exposure and treatment outcomes in non-small-cell lung cancer. *Eur J Cancer* 2019;109:12-20.
31. Kim KH, Cho J, Ku BM, et al. The first-week proliferative response of peripheral blood PD-1(+)CD8(+) T cells predicts the response to anti-PD-1 therapy in solid tumors. *Clin Cancer Res* 2019.
32. Riaz N, Havel JJ, Makarov V, et al. Tumor and Microenvironment Evolution during Immunotherapy with Nivolumab. *Cell* 2017;171:934-49 e16.
33. Hamanishi J, Mandai M, Ikeda T, et al. Safety and Antitumor Activity of Anti-PD-1 Antibody, Nivolumab, in Patients With Platinum-Resistant Ovarian Cancer. *Journal of clinical oncology : official journal of the American Society of Clinical Oncology* 2015;33:4015-22.
34. Matulonis UA, Shapira-Frommer R, Santin A, et al. Antitumor activity and safety of pembrolizumab in patients with advanced recurrent ovarian cancer: Interim results from the phase 2 KEYNOTE-100 study. (Abstract). *Journal of Clinical Oncology* 2018;Suppl5511:5511.

35. Varga A, Piha-Paul SA, Ott PA, et al. Pembrolizumab in patients (pts) with PD-L1–positive (PD-L1+) advanced ovarian cancer: Updated analysis of KEYNOTE-028. (Abstract). *Journal of Clinical Oncology* 2017;Suppl.5513:5513-.
36. Strasser A, Jost PJ, Nagata S. The many roles of FAS receptor signaling in the immune system. *Immunity* 2009;30:180-92.
37. Holler N, Tardivel A, Kovacsovics-Bankowski M, et al. Two adjacent trimeric Fas ligands are required for Fas signaling and formation of a death-inducing signaling complex. *Mol Cell Biol* 2003;23:1428-40.
38. Kischkel FC, Hellbardt S, Behrmann I, et al. Cytotoxicity-dependent APO-1 (Fas/CD95)-associated proteins form a death-inducing signaling complex (DISC) with the receptor. *The EMBO journal* 1995;14:5579-88.
39. Kokkonen TS, Augustin MT, Kokkonen J, Karttunen R, Karttunen TJ. Serum and tissue CD23, IL-15, and FasL in cow's-milk protein-sensitive enteropathy and in coeliac disease. *Journal of pediatric gastroenterology and nutrition* 2012;54:525-31.
40. Kokkonen TS, Karttunen TJ. Endothelial Fas-Ligand in Inflammatory Bowel Diseases and in Acute Appendicitis. *J Histochem Cytochem* 2015;63:931-42.
41. Motz GT, Santoro SP, Wang LP, et al. Tumor endothelium FasL establishes a selective immune barrier promoting tolerance in tumors. *Nature medicine* 2014;20:607-15.
42. Tauzin S, Chaigne-Delalande B, Selva E, et al. The naturally processed CD95L elicits a c-cyes/calcium/PI3K-driven cell migration pathway. *PLoS Biol* 2011;9:e1001090.
43. Poissonnier A, Legembre P. Boyden Chamber Assay to Study of Cell Migration Induced by Metalloprotease Cleaved-CD95L. *Methods Mol Biol* 2017;1557:117-23.
44. Prat J, Oncology FCoG. Staging classification for cancer of the ovary, fallopian tube, and peritoneum. *Int J Gynaecol Obstet* 2014;124:1-5.
45. Hendry S, Salgado R, Gevaert T, et al. Assessing Tumor-infiltrating Lymphocytes in Solid Tumors: A Practical Review for Pathologists and Proposal for a Standardized Method From the International Immunooncology Biomarkers Working Group: Part 1: Assessing the Host Immune Response, TILs in Invasive Breast Carcinoma and Ductal Carcinoma In Situ, Metastatic Tumor Deposits and Areas for Further Research. *Adv Anat Pathol* 2017;24:235-51.
46. Contal C, O'Quigley JQ, J. An application of changepoint methods in studying the effect of age on survival in breast cancer. *Computational Statistics & Data Analysis* 1999;30:252-70.
47. Roy M, Connor J, Al-Niaimi A, Rose SL, Mahajan A. Aldehyde dehydrogenase 1 (ALDH1A1) expression by immunohistochemistry is associated with chemo-refractoriness in patients with high-grade ovarian serous carcinoma. *Hum Pathol* 2017.
48. Luyckx M, Leblanc E, Filleron T, et al. Maximal cytoreduction in patients with FIGO stage IIIC to stage IV ovarian, fallopian, and peritoneal cancer in day-to-day practice: a Retrospective French Multicentric Study. *International journal of gynecological cancer : official journal of the International Gynecological Cancer Society* 2012;22:1337-43.
49. Cowan RA, Eriksson AGZ, Jaber SM, et al. A comparative analysis of prediction models for complete gross resection in secondary cytoreductive surgery for ovarian cancer. *Gynecol Oncol* 2017;145:230-5.
50. Kreso A, Dick JE. Evolution of the cancer stem cell model. *Cell Stem Cell* 2014;14:275-91.
51. Oskarsson T, Batlle E, Massague J. Metastatic stem cells: sources, niches, and vital pathways. *Cell Stem Cell* 2014;14:306-21.

52. Poissonnier A, Sanseau D, Le Gallo M, et al. CD95-Mediated Calcium Signaling Promotes T Helper 17 Trafficking to Inflamed Organs in Lupus-Prone Mice. *Immunity* 2016;45:209-23.
53. Vira H, Pradhan V, Umare V, et al. Role of MMP-7 in the pathogenesis of systemic lupus erythematosus (SLE). *Lupus* 2017;26:937-43.
54. Cancer Genome Atlas Research N. Integrated genomic analyses of ovarian carcinoma. *Nature* 2011;474:609-15.
55. Barbarin A, Cayssials E, Jacomet F, et al. Phenotype of NK-Like CD8(+) T Cells with Innate Features in Humans and Their Relevance in Cancer Diseases. *Front Immunol* 2017;8:316.
56. Barnett JC, Bean SM, Whitaker RS, et al. Ovarian cancer tumor infiltrating T-regulatory (T(reg)) cells are associated with a metastatic phenotype. *Gynecol Oncol* 2010;116:556-62.
57. Hagemann AR, Hagemann IS, Cadungog M, et al. Tissue-based immune monitoring II: multiple tumor sites reveal immunologic homogeneity in serous ovarian carcinoma. *Cancer Biol Ther* 2011;12:367-77.
58. Schiavon V, Duchez S, Branchtein M, et al. Microenvironment tailors nTreg structure and function. *Proc Natl Acad Sci U S A* 2019;116:6298-307.
59. Malleter M, Tauzin S, Bessede A, et al. CD95L cell surface cleavage triggers a prometastatic signaling pathway in triple-negative breast cancer. *Cancer research* 2013;73:6711-21.

Figure legends:

**Figure 1: Serum cleaved CD95L is increased in High grade Serous Ovarian Cancer (HGSOC) patients with better prognosis.**

A, Serum s-CD95L level in all ovarian cancer cohort compared with healthy donor

B, Kaplan-Meier analysis of recurrence ovarian cancer patients with s-CD95L higher (thick line) or lower (dotted line) than 516pg/mL

C, Kaplan-Meier analysis of recurrence in High Grade Serous (HGS) Ovarian Cancer patients with cleaved CD95L higher (thick line) or lower (dotted line) than 516pg/mL.

D, Serum cl-CD95L level according Disease free survival (DFS) (< or > 12 months) in HGS Ovarian Cancer patients

E, Kaplan-Meier analysis of overall survival in High Grade Serous (HGS) Ovarian Cancer patients with cleaved CD95L higher (thick line) or lower (dotted line) than 516pg/mL.

**Figure 2: s-CD95L does not display any functional modifications on HGSOC tumor cells.**

A, CD24 and CD44 expression and ALDH1 activity on different ovarian cancer cells lines with or without s-CD95L (100 ng/mL).

B, Comparison of mRNA level expression of mesenchymal (FAP1, ZEB1, ZEB2, SNAIL, SLUG, TWIST1) or epithelial (CDH1) genes in OVCAR 8 (mesenchymal cell) and OVCAR 3 (epithelial cell). Evaluation of mRNA level expression of mesenchymal (ZEB1, ZEB2, SLUG, TWIST1) or epithelial (CDH1) genes in OVCAR 8 and OVCAR 3 (epithelial cell) with or without s-CD95L (100 ng/mL).

C, Ovarosphere formation on ovarian cancer cells with or without s-CD95L (100 ng/mL).

**Figure 3: concentrations of serum s-CD95L are associated with increased tumor-infiltrating immune cells**

A, Immunohistochemical staining analysis of consecutive sections of high grade serous ovarian cancer tissues stained with markers of blood (CD31+), or lymphatic endothelium (D2-40+) and CD95L. Black arrowheads depict a blood vessel (CD31 staining and CD95L staining) and red arrowheads depict immune cells near vessels. (picture from three patients) (data representative of 37 analyzed patients)

B, Immunohistochemistry of immune cells in tumor sample of high grade serous ovarian cancer patient with high level of s-CD95L (851.57 pg/mL) and low level of s-CD95L (40pg/mL).

**Table 1. Clinical characteristics of patients with high-grade serous ovarian cancer patients according to a serum s-CD95L threshold of 516 pg/mL.**

<b>Variable(s)*</b>	<b>s- CD95L ≥ 516pg/ml n=7</b>	<b>s-CD95L &lt; 516pg/ml n=30</b>	<b>p</b>
Age (years) (mean (± SD))	65.1 ± 11.6	63.3 ± 11.0	0.6002
Menopause			
No	1 (14.3%)	1 (3.8%)	0.3845
Yes	6 (89.7%)	25 (96.2%)	
Missing data	0 (0%)	4 (7.7%)	
Ca125 level (UI/mL) (mean (± SD))	1032 ± 1036	4155 ± 9370	0.6399
FIGO stage			
IIIc	7 (100.0%)	22 (73.3%)	0.4400
IV	0 (0%)	8 (26.7%)	
Nodes Involved			
Yes	2 (28.6%)	14 (46.7%)	<b>0.0409</b>
No	5 (71.4%)	7 (23.3%)	
Not removed	5 (20.8%)	9 (30.0%)	
BRCA gene mutation carrier			
No	2 (28.5%)	9 (30.0%)	0.4231
Yes	1 (14.2%)	1 (3.3%)	
Not known	4 (57.1%)	20 (66.6%)	
Neoadjuvant chemotherapy			
No	1 (14.2%)	9 (30.0%)	0.6471
Yes	6 (85.7%)	21 (70.0%)	
Residual disease after surgery			
No	7 (100.0%)	22 (73.3%)	0.3079
Yes	0 (0.8%)	8 (26.7%)	

SD: Standard deviation; FIGO: International Federation of Gynaecology and Obstetrics; BRCA: Breast Cancer gene

**Table 2. Tumor infiltrating cell count in high-grade serous ovarian carcinoma patients based on immunohistochemical analysis of CD95L expression**

<b>Variable(s)</b>	<b>Endothelial membrane CD95L expression (n=29)</b>	<b>No membrane CD95L expression (n=8)</b>	<b>p</b>
s-CD95L serum level	358.20 ± 350.12	226.04 ± 205.28	0.4485
CD3	9022.7 ± 7832.4	9945.1 ± 13658	0.4277
CD4	3841.0 ± 4760.1	1161.1 ± 935.65	0.1555
CD8	4262.3 ± 5955.5	4187.9 ± 6739.0	0.4719
CD20	2766.7 ± 3933.3	1411.6 ± 2610.8	0.1006
<b>FoxP3</b>	<b>717.62 ± 750.59</b>	<b>276.25 ± 353.65</b>	<b>0.0528</b>
CD163	8809.8 ± 5430.0	9270.6 ± 7968.3	0.5927
IL17	789.03 ± 937.34	545.25 ± 669.34	0.3660
PD-L1	904.41 ± 1360.1	527.63 ± 563.54	0.5927
<b>GRANZYMEB</b>	<b>1722.6 ± 1332.2</b>	<b>762.88 ± 794.99</b>	<b>0.0173</b>

**Table 3. Univariate analysis of risk of recurrence or death**

Data	Risk of recurrence		Risk of death	
	HR [95% CI]	P	HR [95% CI]	P
Age > 65 years	1.03 [0.52–2.06]	0.9332	1.09 [0.52–2.06]	0.8419
Serum Ca125 level (UI/mL) <1200	0.89 [0.42–1.86]	0.7519	0.85 [0.35–2.56]	0.7321
Stage FIGO IV (vs IIIc)	1.50 [0.63–3.56]	0.3583	1.97 [0.77–5.05]	0.2645
Involved nodes				
No	1	<b>0.0209</b>	1	<b>0.0072</b>
Yes	2.08 [0.90–4.82]		2.85 [0.90–9.00]	
Not removed	3.80 [1.48–9.75]		7.03 [2.05–24.12]	
Residual disease after surgery	5.74 [2.40–13.74]	<b>&lt; 0.0001</b>	6.31 [2.40–13.74]	<b>0.0002</b>
Neoadjuvant chemotherapy	1.29 [0.60–13.74]	0.2937	2.69 [0.90–8.04]	0.0762
s-CD95L <516 pg/mL	<b>3.44 [1.29–9.15]</b>	<b>0.0135</b>	<b>4.45 [1.03–19.10]</b>	<b>0.0449</b>
CD3 >6000	<b>0.32 [0.15–3.76]</b>	<b>0.0040</b>	0.28 [0.11–0.70]	<b>0.0061</b>
CD8 >750	0.45 [0.20–1.01]	0.0532	<b>0.35 [0.37–1.68]</b>	<b>0.0242</b>
Granzyme B >1200	1.62 [0.81–3.24]	0.1733	<b>2.52 [1.08–5.92]</b>	<b>0.0335</b>
CD4 >803	0.51 [0.25–1.05]	0.0670	<b>0.42 [0.18–0.99]</b>	<b>0.0468</b>
IL17 >740	1.58 [0.75–3.33]	0.2318	1.14 [0.47–2.81]	0.7687
Foxp3 >700	0.46 [0.21–1.05]	0.0639	0.76 [0.31–1.86]	0.5506
CD163 >5500	0.56 [0.27–1.13]	0.1048	0.62 [0.27–1.43]	0.2577
PD-L1 >1000	0.36 [0.12–1.02]	0.0550	0.37 [0.09–1.60]	0.1858
CD20 >1060	<b>0.39 [0.19–0.82]</b>	<b>0.0134</b>	<b>0.33 [0.13–0.82]</b>	<b>0.0174</b>
Membrane CD95L expression	0.64 [0.31–1.89]	0.2842	0.56 [0.23–1.38]	0.2061

**Table 4. Multivariate analysis of risk of recurrence**

<b>Data</b>	<b>Risk of recurrence HR [95% CI]</b>	<b>P</b>
Residual disease after surgery	<b>6.16 [2.27–16.67]</b>	<b>0.0003</b>
CD3 > 6000	<b>0.34 [0.15–0.79]</b>	<b>0.0124</b>
Granzyme B <1200	<b>2.63 [1.16–5.95]</b>	<b>0.0207</b>
s-CD95L <516 pg/mL	<b>3.54 [1.13–11.11]</b>	<b>0.0301</b>

**Table 5. Multivariate analysis of risk of death**

<b>Data</b>	<b>Risk of death HR [IC95%]</b>	<b>P</b>
Residual disease after surgery	<b>9.99 [2.61–38.19]</b>	<b>0.0035</b>
CD3 >6000	<b>0.27 [0.10–0.71]</b>	<b>0.0082</b>
CD8 >6000	<b>0.33 [0.12–0.87]</b>	<b>0.0252</b>

# Figure 1

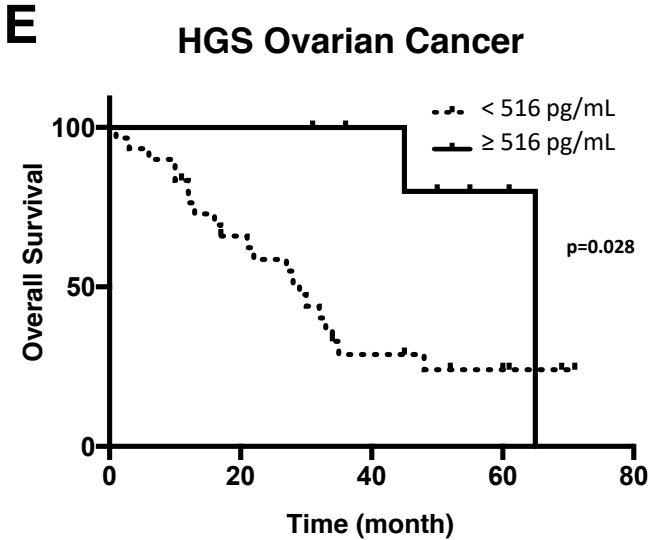
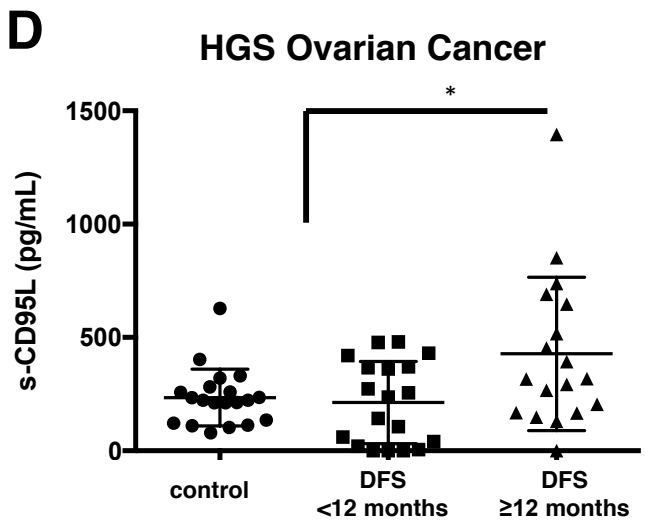
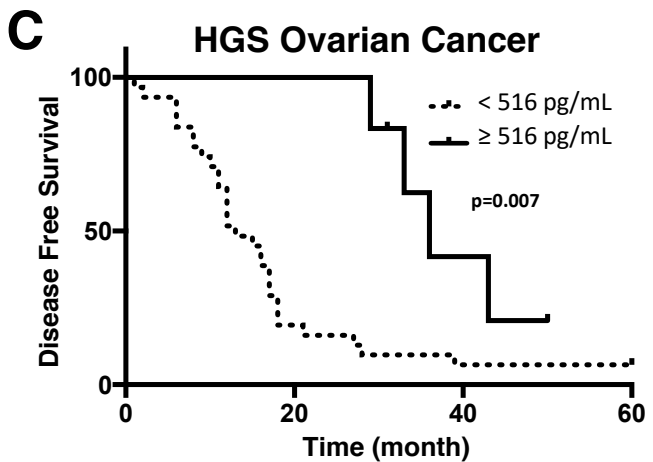
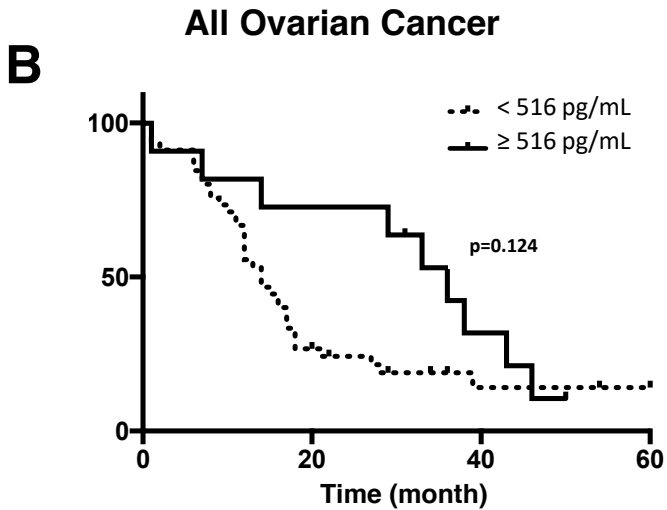
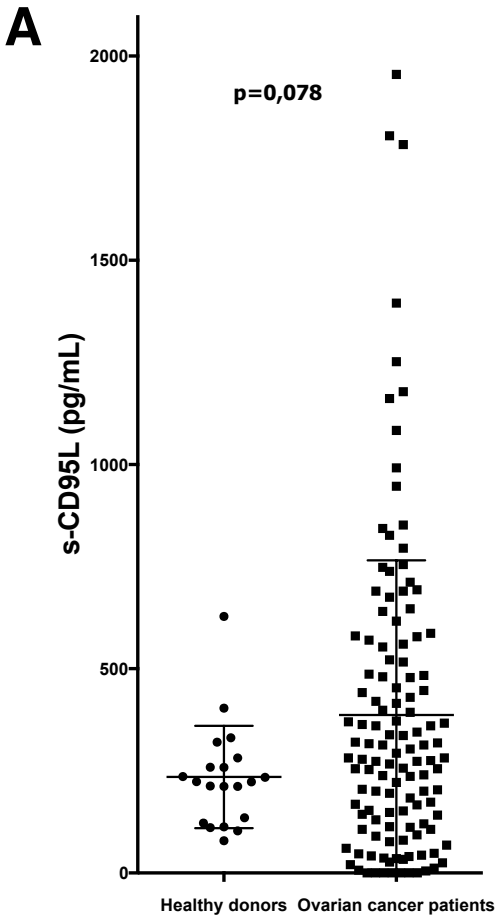
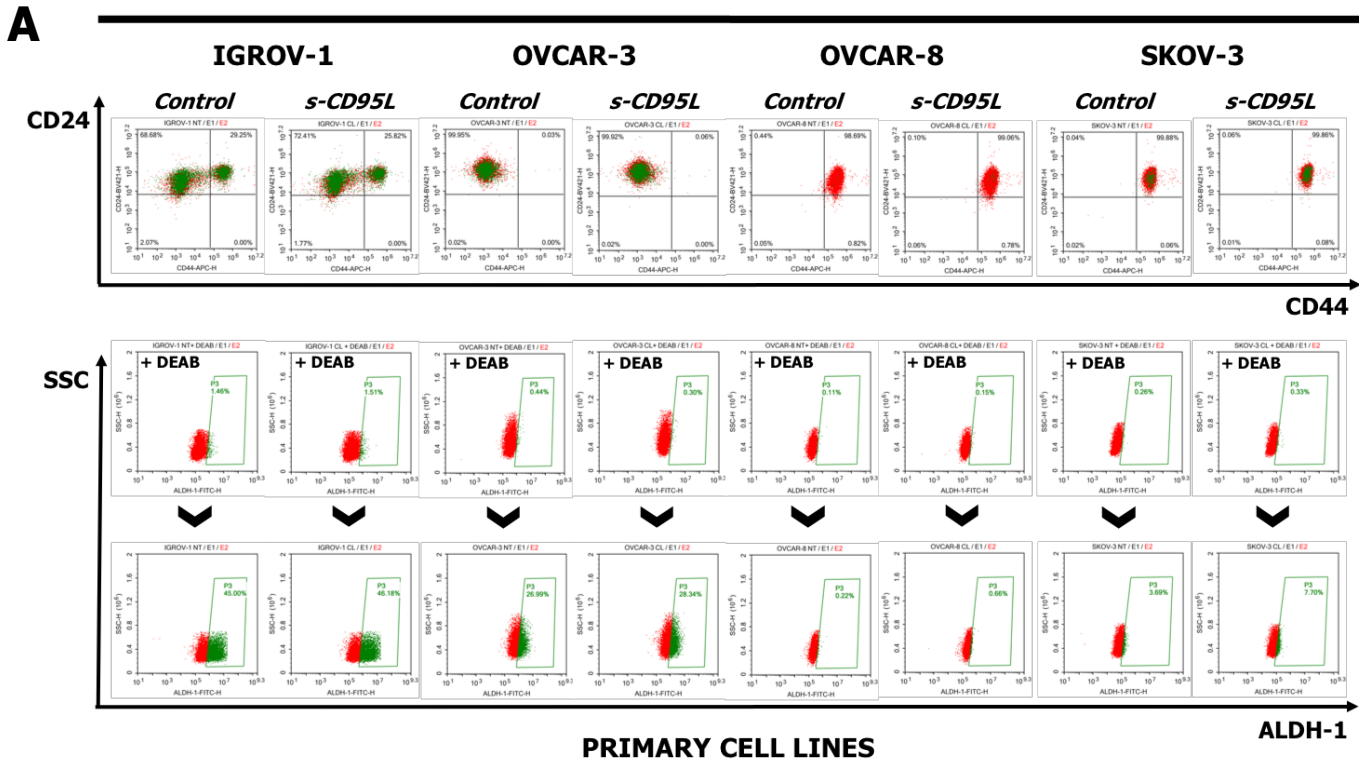
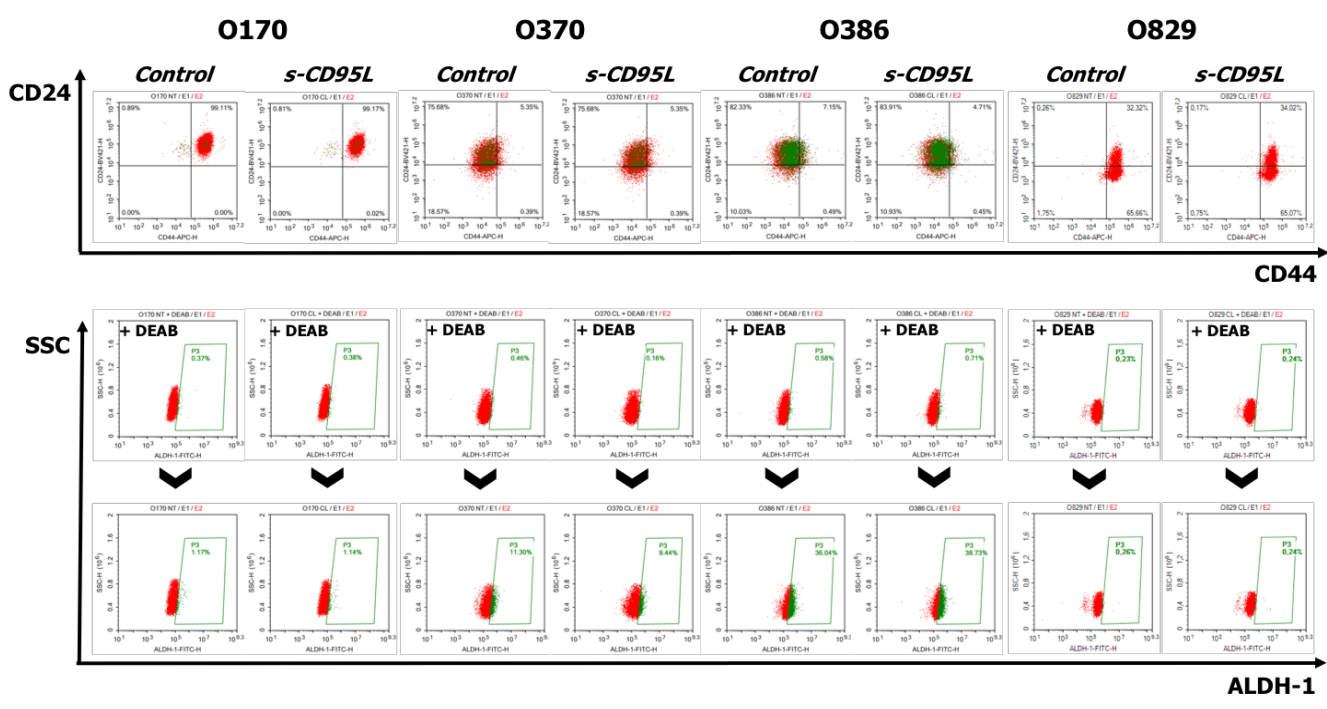


# Figure 2

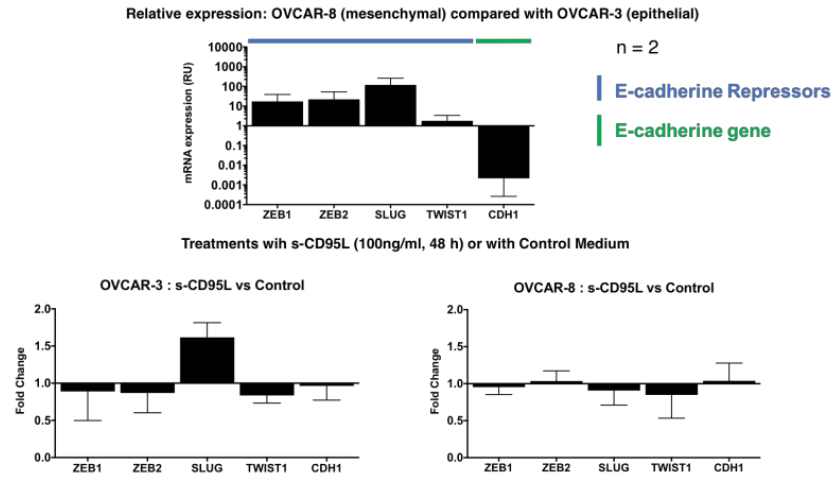
## COMMERCIAL CELL LINES



## PRIMARY CELL LINES



**B**



**C**

## OVCAR 8

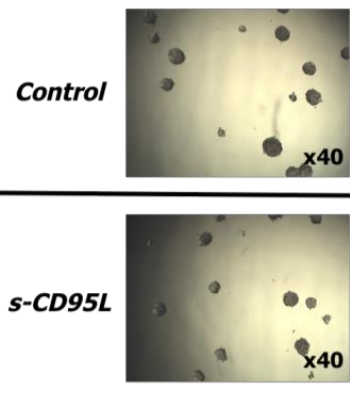


**Figure 3**

